Composites Part B 156 (2019) 108–112

Contents lists available at ScienceDirect

Composites Part B

journal homepage: www.elsevier.com/locate/compositesb

Temperature dependent thermoelectric properties of cuprous delafossite oxides

Yining Feng[a], Aline Elquist[b], Yuepeng Zhang[c], Kaizhong Gao[c], Ian Ferguson[d], Athanasios Tzempelikos[e], Na Lu[a,b,*]

[a] Lyles School of Civil Engineering, Sustainable Materials and Renewable Technology (SMART) Lab, Purdue University, West Lafayette, IN, 47906, USA
[b] School of Materials Engineering, Birck Nanotechnology Center, Purdue University, West Lafayette, IN, 47906, USA
[c] Energy Systems Division, Argonne National Lab, Lemont, IL, 60439, USA
[d] Electrical and Computer Engineering, Missouri University of Science and Technology, Rolla, MO, 65409, USA
[e] Lyles School of Civil Engineering, Center for High Performance Buildings, Ray W. Herrick Laboratories, Purdue University, West Lafayette, IN 47906, USA

ARTICLE INFO

Keywords:
Delafossite oxides
Thermoelectric
Power factor
Power generation

ABSTRACT

The use of nanostructured delafossite oxides in thermoelectric (TE) applications has attracted a great interest due to their high performance and long-term stability at elevated temperatures. Cuprous delafossites, $CuMO_2$ (M = Al, Cr, Fe, Ga, Mn), compared to conventional TE materials, such as Bi_2Te_3, PbTe and SiGe, are non-toxic and more earth abundant. In particular, $CuAlO_2$ compound shows a great potential for high performance thermoelectric materials.

In this work, a systematic study of temperature dependent TE properties of cuprous delafossite materials, $CuAlO_2$, is reported. The optimization of the TE properties has been realized by controlling nanostructure size around 80 nm $CuAlO_2$ powder was prepared using a solid-state synthesis method at ~1373 K in nitrogen/air atmosphere. The nanostructure size was controlled by a high energy ball milling process. Reducing the particle size of nanostructured bulk materials decouples interdependent electron and phonon transport and results in a lattice thermal conductivity decrease without deteriorating electrical conductivity. The high effective mass plays a dominant role in the high Seebeck coefficient and low electrical conductivity. The power factor reached $\sim 0.78 \times 10^{-5}$ W/mK^2 at 780 K. Temperature dependent TE properties, including Seebeck coefficient, electrical conductivity, and thermal conductivity are analyzed. The processing-structure-property correlation of these materials are discussed.

1. Introduction

There is an increasing need to supply clean and renewable energy to fulfill the world's high energy demand. Harvesting waste heat for electricity is one approach to improve sustainability. Thermoelectric materials have the ability to directly convert thermal energy into electricity via Seebeck effect [1–3]. Thermoelectric generators are silent, reliable solid-state devices with no moving parts, making them attractive for other applications, such as power generation in remote environments (e.g. space) or autonomous sensors [4,5]. However, there are still challenges using TE technology for applications. One of biggest challenges is optimized TE properties of existing TE materials since three parameters (S, σ, κ_T) are affected by each other [6]. The quality of materials for TE applications is described by a dimensionless parameter zT [7,8], which is defined as the following:

$$zT = \frac{S^2\sigma}{k_T}T \tag{1}$$

where S is the Seebeck coefficient, σ is the electrical conductivity, k is the thermal conductivity. In physics, κ_T is the sum of the electronic contribution (κ_e, due to carrier transport) and lattice contribution (κ_l, due to phonon transport). The term $S^2\sigma$ is called the power factor (PF). A high PF indicates that a TE power generator can achieve a high power output. In our previous theoretical work, one effective way to improve the TE properties is by using small-nanostructure-size (SNS) limit to reach a high zT [9]. Also, cuprous delafossite oxides are promising candidates for thermoelectric materials due to their electronic properties can be tuned from insulator behavior to metallic behavior by

* Corresponding author. Lyles School of Civil Engineering, Sustainable Materials and Renewable Technology (SMART) Lab, Purdue University, West Lafayette, IN, 47906, USA.
E-mail address: luna@purdue.edu (N. Lu).

https://doi.org/10.1016/j.compositesb.2018.08.070
Received 5 June 2018; Accepted 20 August 2018
Available online 22 August 2018
1359-8368/ Published by Elsevier Ltd.

manipulating their crystal structures, chemical compositions and doping concentrations [10,11].

In 1997, Kawazoe et al. reported the p-type conductivity of transparent thin film $CuAlO_2$ as 1 S/cm at room temperature [12]. Also, the previous study shows $CuAlO_2$ has a relatively large electronic bandgap (~3.4 eV) and flat band structure [13]. Moreover, Hao et al. has conducted a computational-driven TE materials search and identified $CuAlO_2$ is a promising p-type candidate [9]. $CuAlO_2$ has a layered, delafossite structure that can be considered a natural superlattice, which is more stable and easy for synthesis [14]. Superlattice structures show a lot of promise for TE materials [15–17]. Other layered oxide materials used for TE, such as $NaCo_2O_4$ [18], and $SrTiO_3$ [19] have demonstrated relatively large zTs. However, temperature dependent thermoelectric transport properties of $CuAlO_2$ have not been fully exploited in existing literature.

To fill this knowledge gap, we have conducted a systematic study of thermoelectric properties of $CuAlO_2$ with the function of temperatures from 300 K to 780 K. Solid-state synthesis of $CuAlO_2$ created a material with a nanostructured grain size, which affects electrical and thermal conductivity. Cold-pressed pellets kept powder maintained the grain size during the annealing process. Annealing temperature and time were optimized for microstructure, which will significantly affect thermoelectric properties [20]. The effects of different annealing times for $CuAlO_2$, on resulting microstructure, and related thermoelectric properties of $CuAlO_2$ were studied.

1.1. Experimental design

High purity CuO and Al_2O_3 were stoichiometrically mixed with alcohol, and ball milled for 6 h using 3 mm yittria stabilized zirconia grinding media at a 40:1 ratio. The resulting powder was dried in oven at 363 K, then pressed into pellets with 13 mm diameter and 1.5 mm thick at 394 K under 8 Tons for 30 min. The pressed pellets were annealed at 1373 K for 5 h, 8 h and 12 h, respectively, in a combination of nitrogen and ambient environments. All samples were furnace cooled.

The crystal structure, and purity of the samples were analyzed via powder X-ray diffraction (XRD) using a Panalytical Empyrean Powder X-ray Diffractometer at 40 kV, 40 mA with Bragg-Brentano mode with Cu Kα radiation. The diffraction patterns were collected from 10-80° for five times. The average crystalline size of the powders was calculated according to Scherrer's equation. A high-resolution transmission electron microscope (FEI Tecnai F20ST) was used to investigate crystal structure of annealed powders. Seebeck coefficient was determined through a home-built measurement system that applies a temperature gradient through the sample and measures the resulting voltage output as described elsewhere [6,21]. The Seebeck coefficient was calculated from the slope of temperature vs voltage. Electrical conductivity was directly measured by four-probe hall measurement system (Ecopia AHT55T5). The thermal conductivity was determined using transient time-dominant method from the thermal diffusivity and specific heat measured by laser flash method (LFA 467, NETZSCH, Germany). All the thermoelectric properties were measured from 300 K to 780 K in a nitrogen environment.

2. Results and discussion

Fig. 1 shows the results of powder x-ray diffraction patterns for $CuAlO_2$ powder with varying annealing times at 1373 K. It can be seen that higher purity of $CuAlO_2$ powder were obtained annealing at 1373 K for 12 h, due to the complete reaction between CuO and Al_2O_3. The main reactions for the formation of $CuAlO_2$ are: $CuO + Al_2O_3 \rightarrow CuAl_2O_4$ and $CuAl_2O_4 + CuO \rightarrow 2CuAlO_2 + 1/2O_2$. There will be a formation of $CuAl_2O_4$ at annealing temperature between 1173 K and 1273 K. The following reactions will result in impurities of $CuAlO_2$: $CuAlO_2 + O_2 \rightarrow 1/2CuAl_2O_4 + 1/2CuO$ and $CuAl_2O_4 \rightarrow CuAlO_2 + 1/2Al_2O_3 + 1/4O_2$ as shown in XRD pattern with

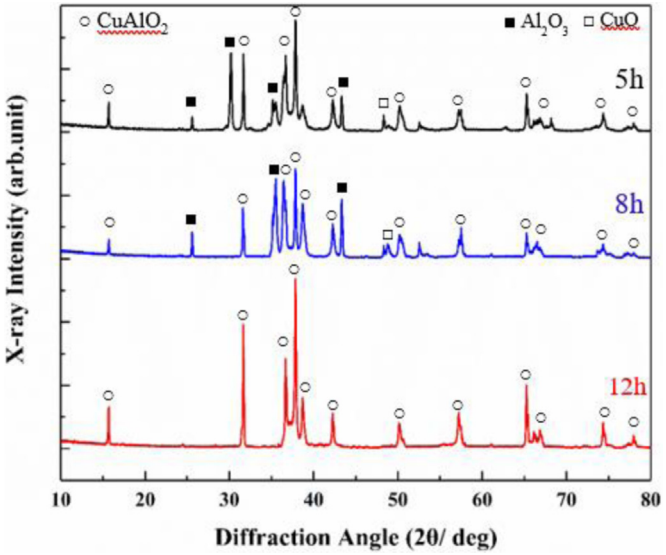

Fig. 1. The XRD patterns of $CuAlO_2$ powder with different annealing time at 1373 K.

CuO and Al_2O_3 peaks. The crystalline structure of the annealed $CuAlO_2$ bodies is rhombohedral, $R\bar{3}m$, a = 2.8567 Å and c = 16.943 Å (JCPDS Card File: 00-035-1401).

Further investigation on microstructure of annealed $CuAlO_2$ powder is done by using high resolution transmission electron microscope (HRTEM). Clear lattice fringes of $CuAlO_2$ is observed as shown in Fig. 2 (a), which indicates high quality of crystal structure. Furthermore, using Fast Fourier Transform (FFT) image obtained by Digital Micrograph software the d-spacing of the lattice orientation was calculated. The d-spacing of the lattice fringes (Fig. 2b) was found to be 2.47 Å, which corresponded to the reported d-value (2.4474 Å) of $(10\bar{1}1)$ plane of r-$CuAlO_2$ (JCPDS Card File: 00-035-1401). The FFT image as shown in Fig. 2c indicates the rhombohedral structure. The HRTEM results are confirmed with an XRD pattern of crystalline structure of r-$CuAlO_2$.

Thermoelectric properties strongly depend on the microstructure of the materials. Fig. 3 shows the temperature dependent Seebeck coefficient of $CuAlO_2$ powder annealing at 1373 K for 12 h. The Seebeck coefficient shows a positive sign over the measured temperature range indicating p-type conductor behavior, which is due to the behavior of hole majority carriers. The Seebeck coefficient increases with the increase of temperature and the highest Seebeck coefficient reaches 665 μV/K at 780 K. No bipolar effect was observed due to the large band gap of $CuAlO_2$ (~3.4eV) [13]. Lu et al. reported the Seebeck coefficient value as 460 μV/K at 780 K for $CuAlO_2$ pellets prepared by SPS method [22], which is lower due to the crystal defects i.e., impurity. Also, the grain size will grow during SPS pressing, which leads to more complicated electron scattering mechanisms. This will affect electrical properties of materials. However, the overall values of Seebeck coefficient for $CuAlO_2$ samples are relatively high. Seebeck coefficient is an intrinsic material property, which measures the thermoelectric voltage induced in response to a temperature difference across the material. High effective mass of the charge carriers will lead to high Seebeck coefficient. The high hole effective mass will increase the density of states at an energy E in the valence band as shown below:

$$g_v(E) = \frac{m_p^* \sqrt{2m_p^*(E_v - E)}}{\pi^2 \hbar^3}, \quad E \le E_v \tag{2}$$

For semiconductors, the relationship among Seebeck coefficient, effective mass and carrier concentration can be expressed below:

$$S = \frac{8\pi^2 k_B^2}{3eh^2} m^* T \left(\frac{\pi}{3n}\right)^{2/3} \tag{3}$$

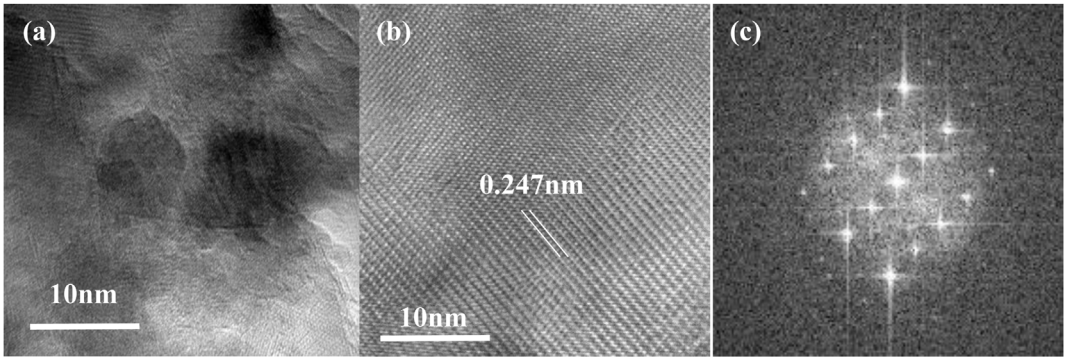

Fig. 2. (a)The HRTEM image of $CuAlO_2$ powder annealing at 1373 K; (b) HRTEM image of an individual grain and (c) FFT pattern.

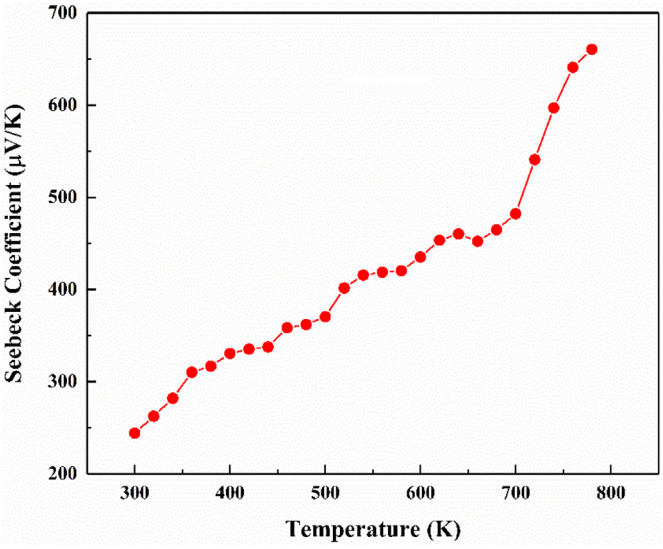

Fig. 3. Temperature dependent Seebeck coefficient of $CuAlO_2$ powder annealing at 1373 K for 12 h.

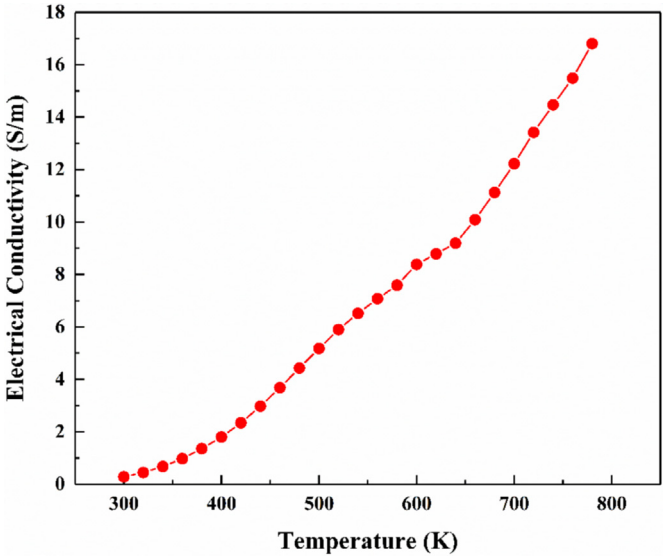

Fig. 4. Temperature dependent electrical conductivity of $CuAlO_2$ powder annealing at 1373 K for 12 h.

where k_B is the Boltzmann constant, e is the carrier charge, h is Planck's constant, m^* is the effective mass of the charger carrier, and n is the carrier concentration. Seebeck coefficient reflects the average entropy transported per charge carrier and thus decreases with increasing carrier as shown in equation (3). Thus, high effective mass and low carrier concentration of the materials are desirable to reach high Seebeck coefficient as shown here.

The Seebeck coefficient is directly related to the density of states, whereas the electrical conductivity can be limited by electronic and morphological defects [23]. Fig. 4 shows the electrical conductivity increases with the temperature increase, which indicates semiconductor behavior. With the increasing temperature thermal energy excites free electrons from the valence band to the conduction band resulting in increased electrical conductivity. The highest electrical conductivity reached is 17 S/m at 780 K. For p-type transparent conductivity oxides (TCOs), those bands are very flat due to the localized oxygen p-type nature of the valence band [24]. P-type TCOs have high hole effective mass. Thus, it is very challenging to reach high electrical conductivity for $CuAlO_2$.

The relationship between electrical conductivity and effective mass is shown below:

$$\sigma = \frac{ne^2\tau}{m^*} \tag{4}$$

As can be seen that high effective mass will result in low mobility, thus the electrical conductivity decreases. To reach high electrical conductivity, higher carrier concentration and lower effective mass are desirable, however it often degenerates the Seebeck coefficient of materials as governed by equation (3). Thus, the investigation of an effective doping mechanism for improving electrical conductivity without degenerating the Seebeck coefficient is crucial to increasing electrical properties of p-type TCOs materials for applications of thermoelectric power generation.

For thermoelectric applications, thermal conductivity (k) is a very important parameter as it determines the efficiency of heat flow through materials and system. Fig. 5 shows the temperature dependent thermal conductivity of the $CuAlO_2$ annealing at 1373 K for 12 h. The value of thermal conductivity is 2.134 W/mK at 780 K. The trend of thermal conductivity increases and then decreases with the temperature increase.

The total thermal conductivity (κ_T) consists of contributions from both electron and phonon transport, defined as following:

$$\kappa_T = \kappa_e + \kappa_l \tag{5}$$

where $\kappa_e$and κ_l are respectively, the electron and lattice thermal conductivity. κ_l is known as the most important mechanism for heat conduction in semiconductors at temperatures close to room temperature, which normally accounts for 90% contributions in wide bandgap materials.

At lower temperatures the thermal conductivity of $CuAlO_2$ is low. Energy and phonon vibrations increase with a temperature increase, which results in an increase of group velocity that enhances thermal conductivity. However, with the temperature increases, more phonon scattering is observed from point defect scattering contributions due to

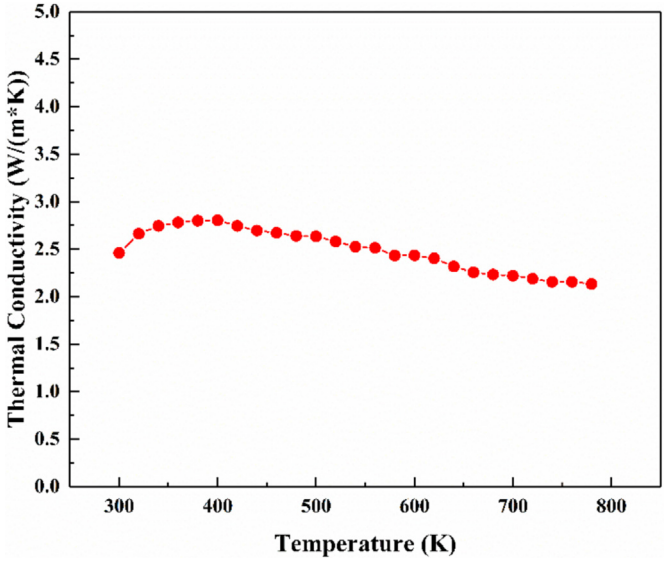

Fig. 5. Temperature dependent thermal conductivity of $CuAlO_2$ powder annealing at 1373 K for 12 h.

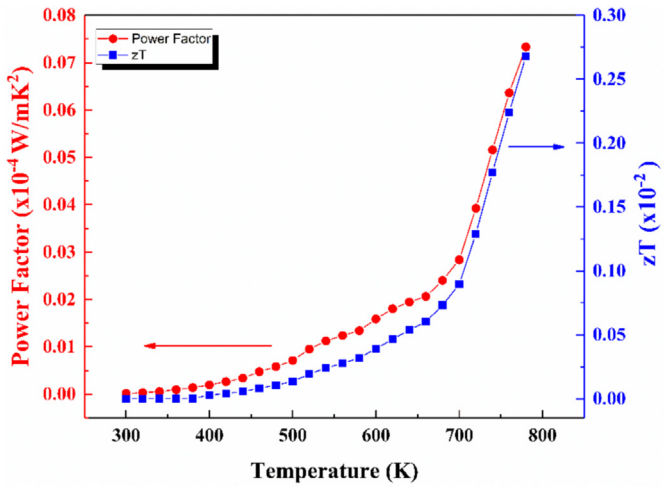

Fig. 6. Power factor and Figure of Merit of $CuAlO_2$ powder.

mass disorder and bond length disorder at higher temperature, and phonon-phonon Umklapp scattering. These phenomena typically lead to a decreased thermal conductivity with the temperature increased as we observed in this study. Thus, one way to decrease the lattice thermal conductivity is to decouple electron and phonon transport using nanostructures to scatter phonons more effectively than electrons, which decreases thermal conductivity without significantly disrupting the electrical conductivity. To achieve this goal, we used cold pressing method to maintain the small nano-grain size (~80 nm) of the ball milled powder, which reduce lattice thermal conductivity without compromising electrical properties as shown in this work.

The power factor ($PF = S\sigma^2$), which is calculated from the data in Figs. 3 and 4, represents the electrical performance of thermoelectric materials, as shown in Fig. 6. The power factor increases as the temperature increases up to 780 K. The value of the power factor at 780 K for $CuAlO_2$ samples is 0.78×10^{-5} W/mK^2. The value of the power factor is indicative of a thermoelectric materials ability to generate electricity, which increases with the temperature.

The quality of materials for TE applications is described by a dimensionless figure of merit, zT. The calculated zT values are shown in Fig. 5. Both electrical and thermal properties will affect materials figure of merit. There are two strategies to improve $CuAlO_2$ zT: (1) to improve the power factor, which requires optimized dopants for $CuAlO_2$ that increases both electrical conductivity and Seebeck coefficient; (2) to reduce the thermal conductivity by using small-nanostructure-size (SNS) limit [9] that requires optimum nanostructure size a is larger than electron mean free path but smaller than phonon mean free path, which results in the increase of phonon scattering without deteriorating electron transport. Thus, lattice thermal conductivity will decrease, and electrical conductivity will maintain high values to reach a high zT.

3. Conclusion

In this work, we have investigated the temperature dependent thermoelectric properties of $CuAlO_2$ with a focus on an optimization of annealing process for improved thermoelectric properties. Both XRD patterns and HRTEM results show high purity and a rhombohedral structure of $CuAlO_2$ powder obtained when annealed at 1373 K for 12 h. The annealing time is one of the key factors for the formation of 3R delafossite phase in $CuAlO_2$. The resulting nanocrystalline $CuAlO_2$ has been characterized both electrical and thermal properties. The value of the Seebeck coefficient is positive over the measured temperature range, which shows p-type behavior, and it increases with the increase of temperature. The electrical conductivity increases as the temperature increases, indicating semiconductor behavior. The high Seebeck coefficient and relatively low electrical conductivity are due to the high effective mass of the charge holes in $CuAlO_2$. Small nano grains in our samples have led to scattering more phonons without deteriorating electrons, which results in low thermal conductivity. The figure of merit is reached at 0.27×10^{-2} at 780 K.

$CuAlO_2$ is a desirable material for mid-high temperature range due to the stability and high Seebeck coefficient, which has a square effect on the power factor. However, the low electrical conductivity limits the broader applications in the thermoelectric field. Thus, an effective doping mechanism for r-$CuAlO_2$ is necessary for future work.

Acknowledgement

The authors at Purdue University are grateful for the financial supports from National Science Foundation CAREER program (under Grants of CMMI – 1560834), Ross Fellowship from Purdue University and Arconic Corporation.

References

[1] Tritt TM. Thermoelectric phenomena, materials, and applications. Annu Rev Mater Res 2011;41:433–48.
[2] Lu N, Ferguson I. III-nitrides for energy production: photovoltaic and thermoelectric applications. Semicond Sci Technol 2013;28:074023.
[3] Hurwitz EN, Asghar M, Melton A, Kucukgok B, Su L, Orocz M, et al. Thermopower study of GaN-based materials for next-generation thermoelectric devices and applications. J Electron Mater 2011;40:513–7.
[4] Alam H, Ramakrishna S. A review on the enhancement of figure of merit from bulk to nano-thermoelectric materials. Nanomater Energy 2013;2:190–212.
[5] Hamid Elsheikh M, Shnawah DA, Sabri MFM, Said SBM, Haji Hassan M, Ali Bashir MB, et al. A review on thermoelectric renewable energy: principle parameters that affect their performance. Renew Sustain Energy Rev 2014;30:337–55.
[6] Hussain B, Akhtar Raja MY, Lu N, Ferguson I. Applications and synthesis of zinc oxide: an emerging wide bandgap material. 2013 high capacit. Opt. Networks emerging/enabling technol. IEEE; 2013. p. 88–93.
[7] Snyder GJ, Toberer ES. Complex thermoelectric materials. Nat Mater 2008;7:105–14.
[8] Tong T, Fu D, Levander AX, Schaff WJ, Pantha BN, Lu N, et al. Suppression of thermal conductivity in in $_x$ Ga $_{1-x}$ N alloys by nanometer-scale disorder. Appl Phys Lett 2013;102:121906.
[9] Hao Q, Xu D, Lu N, Zhao H. High-throughput Z T predictions of nanoporous bulk materials as next-generation thermoelectric materials: a material genome approach. Phys Rev B 2016;93:205206.
[10] Hurwitz EN, Asghar M, Melton A, Kucukgok B, Su L, Orocz M, et al. Thermopower study of GaN-based materials for next-generation thermoelectric devices and applications. J Electron Mater 2011;40:513–7.
[11] Feng Y, Jiang X, Ghafari E, Kucukgok B, Zhang C, Ferguson I, et al. Metal oxides for thermoelectric power generation and beyond. Adv Compos Hybrid Mater 2018;1:114–26.

[12] Kawazoe H, Yasukawa M, Hyodo H, Kurita M, Yanagi H, Hosono H. P-type electrical conduction in transparent thin films of CuAlO2. Nature 1997;389:939–42.
[13] Gillen R, Robertson J. Band structure calculations of CuAlO 2, CuGaO 2, CuInO 2, and CuCrO 2 by screened exchange. Phys Rev B 2011;84:035125.
[14] Ishiguro T, Kitazawa A, Mizutani N, Kato M. Single-crystal growth and crystal structure refinement of CuAlO2. J Solid State Chem 1981;40:170–4.
[15] Hicks LD, Dresselhaus MS. Use of quantum-well superlattices to obtain a high figure of merit from nonconventional thermoelectric materials. MRS Proc 1993;326:413.
[16] Koumoto K, Wang Y, Zhang R, Kosuga A, Funahashi R. Oxide thermoelectric materials: a nanostructuring approach. Annu Rev Mater Res 2010;40:363–94.
[17] Harman TC, Taylor PJ, Walsh MP, LaForge BE. Quantum dot superlattice thermoelectric materials and devices. Science 2002;297:2229–32.
[18] Terasaki I, Sasago Y, Uchinokura K. Large thermoelectric power in $NaCo_2O_4$ single crystals. Phys Rev B 1997;56:R12685–7.
[19] Ohta H, Sugiura K, Koumoto K. Recent progress in oxide thermoelectric materials: p-type $Ca_3Co_4O_9$ and n-type $SrTiO_3$. Inorg Chem 2008;47:8429–36.
[20] Lu N, Oza S. Thermal stability and thermo-mechanical properties of hemp-high density polyethylene composites: effect of two different chemical modifications. Compos B Eng 2013;44:484–90.
[21] Lu N, Zhou C, Wang Y, Elquist AM, Ghods A, Ferguson IT, et al. A review of earth abundant ZnO-based materials for thermoelectric and photovoltaic applications. In: Teherani FH, Look DC, Rogers DJ, editors. Oxide-based mater. Devices IX. vol. 10533. SPIE; 2018. p. 53.
[22] Lu Y, Nozue T, Feng N, Sagara K, Yoshida H, Jin Y. Fabrication of thermoelectric CuAlO2 and performance enhancement by high density. J Alloy Comp 2015;650:558–63.
[23] Dresselhaus MS, Chen G, Tang MY, Yang RG, Lee H, Wang DZ, et al. New directions for low-dimensional thermoelectric materials. Adv Mater 2007;19:1043–53.
[24] Zhang KHL, Xi K, Blamire MG, Egdell RG. *P* -type transparent conducting oxides. J Phys Condens Matter 2016;28:383002.